ARTICLES

Formation of CH_3CFCl^+ from Photoionization of CH_3CFCl_2: An Application of Threshold Photoelectron Photoion Coincidence (TPEPICO) Technique

Su-Yu Chiang*

Synchrotron Radiation Research Center, No. 1, R&D Road VI, Hsinchu Science-Based Industrial Park, Hsinchu 300, Taiwan

Yu-Chang Lee and Yuan-Pern Lee

Department of Chemistry, National Tsing Hua University, 101, Sec. 2, Kuang Fu Road, Hsinchu 30013, Taiwan

Received: August 8, 2000

The dissociation of energy-selected $CH_3CFCl_2^+$ to form CH_3CFCl^+ was studied with a molecular-beam/threshold-photoelectron-photoion-coincidence system using synchrotron radiation for ionization. Maximal releases of kinetic energy in the channel $CH_3CFCl^+ + Cl$ at five photon energies were determined from half-widths of CH_3CFCl^+ time-of-flight peaks in coincidence mass spectra. A thermochemical threshold for this channel was determined to be 11.10 ± 0.09 eV after taking kinetic energy releases into account. With this threshold and heats of formation of Cl and CH_3CFCl_2, we derived $\Delta_f H_0^\circ(CH_3CFCl^+) = 149.0 \pm 2.1$ kcal mol^{-1}. Ab initio calculations were also performed to predict heats of formation of CH_3CFCl_2, CH_3CFCl, and their corresponding cations. Our experimental results agree satisfactorily with calculations. On the basis of experimental and theoretical results, we construct an energy diagram for dissociative photoionization of CH_3CFCl_2 to form $CH_3CFCl^+ + Cl$.

1. Introduction

CH_3CFCl_2 (HCFC-141b) is used widely to replace $CFCl_3$ (CFC-11) and $CFCl_2CF_2Cl$ (CFC-113) in industrial applications.[1,2] With increased concern over its impact on atmospheric chemistry, investigations on CH_3CFCl_2 become important. There are numerous reports on ultraviolet (UV) absorption cross sections[3−5] and photodissociation of CH_3CFCl_2,[6,7] as well as reaction kinetics of CH_3CFCl_2 with OH,[3,8−10] $O(^1D)$,[11] and Cl,[12−16] but little is known about thermochemical properties of CH_3CFCl_2 and its related photoproducts, despite their importance in relation to the chemical reactivity of CH_3CFCl_2.

We measured the threshold photoelectron spectrum (TPES) and photoionization mass spectra (PIMS) of CH_3CFCl_2.[17] Valence ionic states were assigned on comparison of experimental vertical ionization energies in the TPES with theoretically predicted values. Three major fragments, CH_3CFCl^+, CH_2CCl^+, and CH_2CF^+, were observed in the PIMS experiment; their respective appearance energies (AE) were determined from the onsets of the photoionization efficiency curves. The parent ion $CH_3CFCl_2^+$ is absent. The AE value of 11.33 ± 0.02 eV for production of CH_3CFCl^+ is nearly identical to the nominal ionization threshold of 11.28 ± 0.02 eV for CH_3CFCl_2 in the TPES. Lack of parent ion and an onset for production of CH_3CFCl^+ similar to that for ionization of CH_3CFCl_2 imply that an unstable $CH_3CFCl_2^+$ dissociates to form CH_3CFCl^+. Moreover, substantial kinetic energy is expected to be released on the dissociative photoionization process.

Kinetic energy released after dissociative photoionization is not taken into account in determination of AE from PIMS experiments; the resulting AE thus represents an upper limit.[18,19] Heats of formation reported previously[17] for three major fragments observed after photoionization of CH_3CFCl_2 suffer from such uncertainty. In analysis of threshold photoelectron photoion coincidence (TPEPICO) spectra, we can take release of kinetic energy into account and thereby determine accurate AE of dissociative photoionization channels.[20−22] Recently, Evans et al.[22] directly determined a thermochemical threshold on dissociative photoionization in the process $SF_6 + h\nu \rightarrow SF_5^+ + F + e^-$ with high-resolution TPEPICO, and they reported an accurate value of $\Delta_f H_0^\circ(SF_5^+)$ that is consistent with theoretical predictions.[23,24] Lack of SF_6^+ upon photoionization of SF_6 is a behavior similar to that of CH_3CFCl_2.

In our investigation of dissociative photoionization of CH_3CFCl_2, TPEPICO mass spectra of CH_3CFCl_2 were recorded at various photon energies near the appearance onset of CH_3CFCl^+. We determined a thermochemical threshold for the dissociative photoionization channel $CH_3CFCl^+ + Cl$ to derive $\Delta_f H_0^\circ(CH_3CFCl^+)$ and a maximal release of kinetic energy at the appearance onset of CH_3CFCl^+. We also performed ab initio calculations to predict enthalpy changes of three isodesmic reactions, ionization energies of CH_3CFCl_2 and CH_3CFCl, and accordingly predicted heats of formation of CH_3CFCl_2, CH_3CFCl, and their corresponding cations. On the basis of experi-

* Corresponding author. Tel: (886)3-578-0281, ext. 7315. Fax: (886)3-578-9816. E-mail: schiang@srrc.gov.tw.

10.1021/jp002823g CCC: $20.00
Published on Web 02/06/2001

mental and theoretical results, we discuss the $CH_3CFCl^+ + Cl$ channel in photoionization of CH_3CFCl_2.

2. Experiment and Calculations

2.1. Experiment. Coincidence measurements were performed with a molecular-beam/threshold-photoelectron-photoion-coincidence (MB/TPEPICO) apparatus, described in detail elsewhere.[25] In brief, synchrotron radiation from the 1.5 GeV electron storage ring at the Synchrotron Radiation Research Center (SRRC) in Taiwan is dispersed with a 1 m Seya-Namioka monochromator having a 1200 lines/mm grating to cover an energy range of 11−12 eV. A resolution of ∼0.02 eV and a photon flux of $>10^9$ photons s^{-1} were achieved when both entrance and exit slits were set at 0.1 mm. Absolute photon energies were calibrated to within ± 0.003 eV on measurement of well-characterized Rydberg peaks in the TPES spectra of Ar and Kr.

In the ionization chamber, the monochromatic vacuum ultraviolet (VUV) radiation intersected perpendicularly with a molecular beam, formed on expanding a CH_3CFCl_2/He mixture through a nozzle and two skimmers. The total stagnation pressure was ∼290 Torr, with a seed ratio of ∼10%. A threshold photoelectron spectrometer and a time-of-flight (TOF) mass spectrometer of Wiley−McLaren type were mounted in opposite directions to measure threshold electrons and ions, respectively; dual microchannel plates served as detectors in both spectrometers. Axes of both spectrometers were perpendicular to those of molecular and photon beams. To improve instrumental resolutions and efficiency of ion collection, a pulsed field of 40 V cm^{-1} with a duration of 30 μs was applied to extract ions whereas electrons were accelerated with a dc field of 1.64 V cm^{-1} before detection.

Signals of detected threshold electrons and ions were fed into a time-to-digital converter (TDC) to record flight durations of ions that were detected within 30 μs of each cycle triggered with a threshold electron. TOF distributions of ions in coincidence with triggering threshold electrons were obtained after $(5-15) \times 10^5$ cycles depending on coincident ion counts. Because synchrotron radiation was operated at a repetition rate of ∼500 MHz, each measured coincidence spectrum has a large contribution from uncorrelated ions piling up in the interaction region. To eliminate such a contribution, a second coincidence spectrum triggered with a signal generated randomly relative to the preceding threshold electron signal was accumulated following each threshold electron-triggered coincidence cycle. Subtraction of the randomly generated coincidence spectrum from the electron-triggered coincidence spectrum yielded a true coincidence spectrum. All data acquisition was controlled with a computer via CAMAC interface, and output from the TDC converter was transferred to the computer for further processing.

CH_3CFCl_2 (Darkin Corp., 99.9%) was degassed with several freeze−pump−thaw cycles before use. Helium (>99.999%), krypton (>99.99%), and argon (>99.99%) were used without further purification.

2.2. Theoretical Calculations. We calculated ionization energies of CH_3CFCl_2 and CH_3CFCl and enthalpy changes of isodesmic reactions related to formation of these two molecules with the GAUSSIAN 98 program.[26] The equilibrium structures were fully optimized using Schegel's analytical gradient method[27] with a B3LYP density functional[28,29] which is a combination of Slater exchange, Becke exchange,[30] and Lee−Yang−Parr (LYP) correlation functionals.[31] Standard basis sets 6-31+G-(d) and aug-cc-pVTZ,[32] a Dunning's correlation-consistent polarized valence triple-ζ basis set augmented with s, p, d, and f diffuse functions, were used in all structural optimization and calculations of vibrational frequencies.

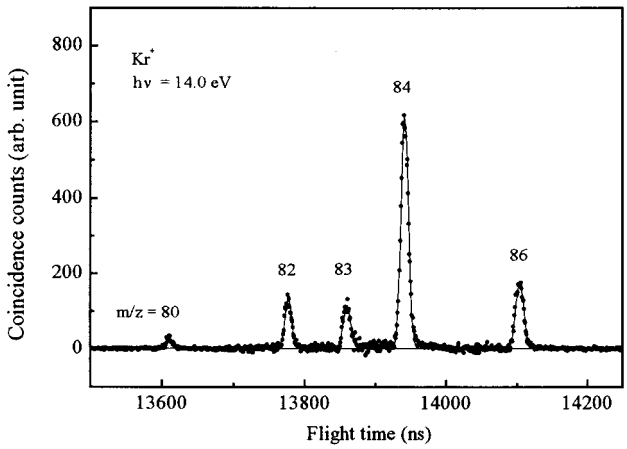

Figure 1. Coincidence TOF spectrum of Kr excited at photon energy 14.0 eV.

The G3B3 theory[33] is based on B3LYP/6-31G(d) geometry and zero-point energies scaled by 0.96. All other steps remain the same as G3 theory except values of higher-level correction parameters, $A = 6.760$ mhartree, $B = 3.233$ mhartree, $C = 6.786$ mhartree, and $D = 1.269$ mhartree. This G3B3 theory was used to calculate the ionization energy and to predict the heat of formation of CH_3CFCl_2 and CH_3CFCl via isodesmic reactions in which the types and number of bonds are the same for products and reactants.

3. Results and Discussion

3.1. Coincidence TOF Spectra for CH_3CFCl^+. Coincidence TOF spectra for helium, argon, and krypton excited at photon energies near their ionization thresholds were recorded to calibrate ion flight times and to verify the effect of kinetic energy release on TOF bandwidths upon dissociation. A coincidence spectrum of krypton excited at 14.0 eV is shown in Figure 1; five TOF peaks correspond to krypton isotopes at $m/z = 80$, 82, 83, 84, and 86. Each peak in this coincidence spectrum was fitted to a Gaussian profile with a full width at half-maximum (fwhm) of ∼12 ns, indicating a small transverse velocity of the skimmed molecular beam along the detection axis. Observed flight times of 3218 (He^+), 9689 (Ar^+), 13610 ($^{80}Kr^+$), 13776 ($^{82}Kr^+$), 13859 ($^{83}Kr^+$), 13941 ($^{84}Kr^+$), and 14103 ns ($^{86}Kr^+$) were fitted to an equation

$$T_0 = 1496.5\,(m/z)^{1/2} + 225.3 \qquad (1)$$

in which T_0 is ion flight time in ns. Flight times calculated with eq 1 agree within 1 ns of experimental values.

Coincidence TOF spectra of CH_3CFCl_2 excited above appearance onset of CH_3CFCl^+ at 11.33 eV were recorded at photon energies of 11.42, 11.52, 11.62, 11.72, and 11.82 eV with 1 ns resolution and corrected for false coincidence background. Corrected coincidence spectra in the region of having ion coincident counts obtained after excitation of CH_3CFCl_2 at photon energies of 11.52, 11.62, and 11.72 eV are shown in Figure 2a−c; all spectra are normalized to an observed maximal intensity. All spectra consist of two partially overlapping, symmetrically broadened, and nearly flat-topped TOF peaks. The intensity ratios of these two TOF peaks are near the $^{35}Cl/^{37}Cl$ isotopic ratio of ∼3, and their respective fwhm are greater than 150 ns. We assigned these two TOF peaks as CH_3-

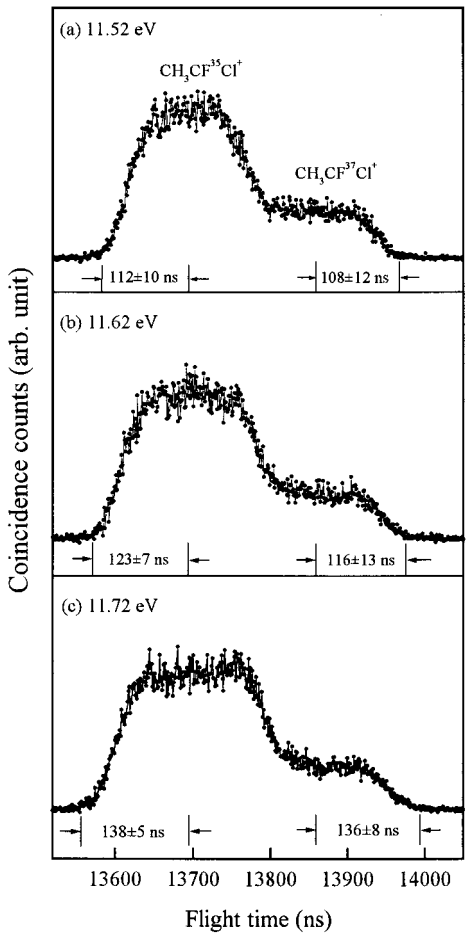

Figure 2. Coincidence TOF spectra of CH_3CFCl_2 excited at photon energies (a) 11.52, (b) 11.62, and (c) 11.72 eV.

$CF^{35}Cl^+$ ($m/z = 81$) and $CH_3CF^{37}Cl^+$ ($m/z = 83$) on the basis of observed flight times and their intensity ratio.

3.2. Thermochemistry of the CH_3CFCl^+ + Cl Channel. The maximal releases of kinetic energy with respect to the center of mass (KE_{CM}) of CH_3CFCl^+ were derived from forward half-widths of $CH_3CF^{35}Cl^+$ TOF peaks and backward half-widths of $CH_3CF^{37}Cl^+$ TOF peaks in the coincidence spectra measured at five photon energies. The full width of a TOF peak corresponds to the turnaround period of the most energetic ion moving away from the TOF ion detector; the analysis of half-widths is required due to overlapping $CH_3CF^{35}Cl^+$ and $CH_3CF^{37}Cl^+$ TOF peaks. We calculated $T_0 = 13694$ and 13859 ns from eq 1 for $CH_3CF^{35}Cl^+$ and $CH_3CF^{37}Cl^+$; half-widths of $CH_3CF^{35}Cl^+$ and $CH_3CF^{37}Cl^+$ TOF peaks subsequently yield KE_{CM} for CH_3CFCl^+ and total kinetic energy releases (KE_T) for a channel of formation of CH_3CFCl^+ according to the following equations:

$$KE_{CM}(CH_3CFCl^+) = [1/(2M_{CH_3CFCl})](\Delta t q V)^2 \qquad (2)$$

in which $M_{CH_3CFCl} = 81$ or 83 g mol^{-1}, Δt is the half-width of the corresponding TOF peak, q is the charge of CH_3CFCl^+, and $V = 41.64$ V cm^{-1} is the electric field, and

$$KE_T = KE_{CM}(CH_3CFCl^+)(M_{CH_3CFCl_2}/M_{Cl}) \qquad (3)$$

in which $M_{CH_3CFCl_2} = 116$ or 118 or 120, and $M_{Cl} = 35$ or 37 g mol^{-1}.

We assume that bond energies and rates of bond breaking of C−^{35}Cl and C−^{37}Cl are the same as those in the calculations of KE_T, although formation of $CH_3CF^{35}Cl^+$ is due to loss of ^{35}Cl from $CH_3CF^{35}Cl^{35}Cl^+$ and loss of ^{37}Cl from $CH_3CF^{35}Cl^{37}Cl^+$. Because $CH_3CF^{35}Cl^+$ TOF peaks originating from such an isotopic effect are unresolved, KE_T for losses of ^{35}Cl and ^{37}Cl at one-photon energy were calculated from eq 3, and their average value was adopted for formation of $CH_3CF^{35}Cl^+$. The uncertainty of this treatment, less than 0.02 eV, is smaller than that of 0.09 eV from determination of half-widths of $CH_3CF^{35}Cl^+$ TOF peaks. The $CH_3CF^{37}Cl^+$ TOF peaks resulting from loss of ^{35}Cl from $CH_3CF^{35}Cl^{37}Cl^+$ and loss of ^{37}Cl from $CH_3CF^{37}Cl^{37}Cl^+$ were analyzed in a similar way. The determined half-widths for TOF peaks of $CH_3CF^{35}Cl^+$ and $CH_3CF^{37}Cl^+$, and corresponding KE_T derived at five photon energies, are listed in Table 1.

AE values for the CH_3CFCl^+ + Cl channel at five photon energies were determined by subtracting corresponding KE_T from photon energy; they are also listed in Table 1. An average value of 11.10 ± 0.09 eV is derived for the $CH_3CF^{35}Cl^+$ + ^{35}Cl/^{37}Cl channel, whereas a value of 11.13 ± 0.16 eV is derived for the $CH_3CF^{37}Cl^+$ + ^{35}Cl/^{37}Cl channel. Listed errors are mainly due to uncertainties on determination of half-widths. The values of AE for both channels agree satisfactorily, except that the determined AE from the latter channel suffers from large errors because of small $CH_3CF^{37}Cl^+$ signals. Thus, we adopted AE = 11.10 ± 0.09 eV. The AE is the thermochemical threshold of the CH_3CFCl^+ + Cl channel if no reverse barrier exists for this process; accordingly $KE_T = 0.23$ eV at the appearance onset of CH_3CFCl^+ was derived on subtraction of the determined AE from the appearance onset of 11.33 eV of CH_3CFCl^+ determined in a PIMS experiment.[17]

The determined AE relates the heats of formation of CH_3CFCl^+, Cl, and CH_3CFCl_2:

$$AE = \Delta_f H_0^\circ(CH_3CFCl^+) + \Delta_f H_0^\circ(Cl) - \Delta_f H_0^\circ(CH_3CFCl_2) - E_{int} \qquad (4)$$

in which $\Delta_f H_0^\circ$ is the heat of formation at 0 K and E_{int} is the average internal energy of CH_3CFCl_2. Thus, to derive $\Delta_f H_0^\circ(CH_3CFCl^+)$ from eq 4 with the determined AE value, $\Delta_f H_0^\circ(Cl)$ and $\Delta_f H_0^\circ(CH_3CFCl_2)$ are required. E_{int} is neglected because CH_3CFCl_2 is cooled in the molecular beam. A literature value for $\Delta_f H_0^\circ(Cl)$ is 28.6 kcal mol^{-1}.[34] Although an experimental value for $\Delta_f H_0^\circ(CH_3CFCl_2)$ is unavailable, we estimate it by interpolation with a nonlinear fit of literature values of $\Delta_f H_{298}^\circ$ for CH_3CCl_3, CH_3CF_2Cl, and CH_3CF_3. Values of $\Delta_f H_{298}^\circ$ for CH_3CCl_3, CH_3CF_2Cl, and CH_3CF_3 are −34.54, −128.09, and −178.86 kcal mol^{-1}, respectively;[34] an estimated $\Delta_f H_{298}^\circ(CH_3CFCl_2)$ is −80.1 kcal mol^{-1}. We tested this method for analogous compounds in two series, CHF_xCl_{3-x} and CF_xCl_{3-x} ($x = 0-3$),[35] and found the variation between literature and fitted values to be less than 0.16 kcal mol^{-1}. Hence, $\Delta_f H_0^\circ(CH_3CFCl_2) = -78.4$ kcal mol^{-1} was derived after correction of $\Delta_f H_{298}^\circ(CH_3CFCl_2)$ using experimental vibrational frequencies of 3028, 3012, 2954, 1442, 1442, 1385, 1159, 1119, 1092, 926, 750, 591, 432, 398, 380, 291, 262, and 248 cm^{-1} for CH_3CFCl_2.[36] Accordingly, $\Delta_f H_0^\circ(CH_3CFCl^+) = 149.0 \pm 2.1$ kcal mol^{-1} was derived from eq 4.

3.3. Theoretical Predictions. We employed theoretical calculations with the G3B3 method to derive $\Delta_f H_0^\circ$ for CH_3CFCl_2, CH_3CFCl, and their corresponding cations. Structures of CH_3CFCl_2, $CH_3CFCl_2^+$, CH_3CFCl, and CH_3CFCl^+ optimized with B3LYP method are shown in Figure 3. Results using the aug-cc-pVTZ basis set are listed, whereas those using the 6-31+G(d) basis set are listed in parentheses for comparison.

TABLE 1: Half-Widths ($\Delta t_{half-width}$) of $CH_3CF^{35}Cl^+$ and $CH_3CF^{37}Cl^+$ TOF Peaks, Total Kinetic Energy Release (KE_T), and Appearance Energy (AE) Measured at Five Photon Energies (PE) near the Appearance Onset of CH_3CFCl^+

	$CH_3CF^{35}Cl^+$			$CH_3CF^{37}Cl^+$		
PE/eV	$\Delta t_{half-width}$/ns	KE_T/eV	AE/eV	$\Delta t_{half-width}$/ns	KE_T/eV	AE/eV
11.42	99 ± 9	0.33 ± 0.05	11.09 ± 0.05	102 ± 9	0.35 ± 0.06	11.07 ± 0.06
11.52	112 ± 10	0.42 ± 0.07	11.10 ± 0.07	108 ± 12	0.39 ± 0.09	11.13 ± 0.09
11.62	123 ± 7	0.50 ± 0.07	11.12 ± 0.07	116 ± 13	0.44 ± 0.11	11.18 ± 0.11
11.72	138 ± 5	0.63 ± 0.04	11.09 ± 0.04	136 ± 8	0.61 ± 0.07	11.11 ± 0.07
11.82	144 ± 6	0.70 ± 0.05	11.12 ± 0.05	142 ± 7	0.67 ± 0.06	11.15 ± 0.06
			Av. 11.10 ± 0.09			Av. 11.13 ± 0.16

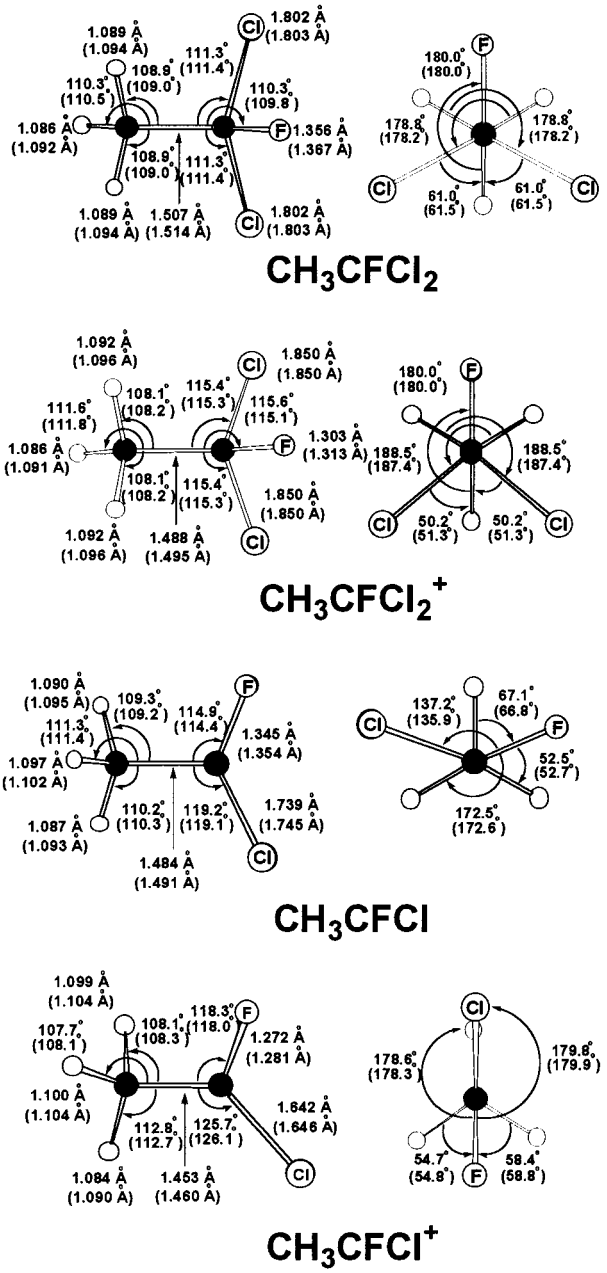

Figure 3. Structures of CH_3CFCl_2, $CH_3CFCl_2^+$, CH_3CFCl, and CH_3CFCl^+ optimized with B3LYP/aug-cc-pVTZ method; results using 6-31+G(d) basis sets are listed in parentheses.

For enthalpy changes ($\Delta H°$) of three isodesmic reactions and ionization energies (IE) of CH_3CFCl_2 and CH_3CFCl, Table 2 lists resultant $\Delta H°$ or IE, literature values[34,35] of $\Delta_f H_0^\circ$ for species relevant to calculations, and derived $\Delta_f H_0^\circ$ for species of interest.

In Table 2, the enthalpy change $\Delta H°$ for the isodesmic reaction

$$CH_2ClCH_2Cl + {}^1/_4CF_4 \rightarrow CH_3CFCl_2 + {}^1/_4CH_4 \quad (5)$$

was calculated to be 2.0 kcal mol^{-1}, consequently $\Delta_f H_0^\circ$ (CH_3CFCl_2) = −78.4 kcal mol^{-1} was derived using literature values[34,35] of $\Delta_f H_0^\circ$ for CH_2ClCH_2Cl, CF_4, and CH_4. Similarly, we derive $\Delta_f H_0^\circ(CH_3CFCl_2)$ = −77.4 kcal mol^{-1} from an isodesmic reaction in which calculated $\Delta H°$ is −6.4 kcal mol^{-1}.

$$C_2H_6 + {}^1/_2CCl_4 + {}^1/_4CF_4 \rightarrow CH_3CFCl_2 + {}^3/_4CH_4 \quad (6)$$

The average value of −77.9 kcal mol^{-1} was used for $\Delta_f H_0^\circ$ (CH_3CFCl_2). This value varies by only 1 kcal mol^{-1} from a value of −76.93 kcal mol^{-1} derived with the ab initio BAC-MP4 method[37] and 0.5 kcal mol^{-1} from a value of −78.4 kcal mol^{-1} estimated from interpolation of $\Delta_f H_{298}^\circ$ of $CH_3CF_xCl_{3-x}$ (x = 0−3), as described above. In addition, IE of CH_3CFCl_2 was calculated to be 255.1 kcal mol^{-1}, and accordingly $\Delta_f H_0^\circ$ ($CH_3CFCl_2^+$) = 177.2 kcal mol^{-1} was derived.

Also listed in Table 2, calculation on the isodesmic reaction

$$CH_3CH_2 + {}^1/_4CCl_4 + {}^1/_4CF_4 \rightarrow CH_3CFCl + {}^1/_2CH_4 \quad (7)$$

yields $\Delta H° = -0.4$ kcal mol^{-1}. Combining this $\Delta H°$ with literature values[34,35] of $\Delta_f H_0^\circ$ for CH_3CH_2, CCl_4, CF_4, and CH_4, we derive $\Delta_f H_0^\circ(CH_3CFCl) = -22.3$ kcal mol^{-1}. An IE of 173.8 kcal mol^{-1} for CH_3CFCl was also calculated, then $\Delta_f H_0^\circ(CH_3CFCl^+)$ was derived to be 151.5 kcal mol^{-1}. This value is near the experimental value of 149.0 ± 2.1 kcal mol^{-1} determined in this work.

Curtiss et al. made test calculations on dissociation energies, IE, and electron affinities using G3, G3(MP2), and G3(MP3) methods on 376 energies, and they found that the average absolute deviations of calculated values from experimental values are 1.07, 1.31, and 1.27 kcal mol^{-1}, respectively.[38] The uncertainty associated with calculations on isodesmic reactions is typically ±1 kcal mol^{-1}. Thus, our experimental value of 149.0 ± 2.1 kcal mol^{-1} for $\Delta_f H_0^\circ(CH_3CFCl^+)$ agrees with the theoretical value of 151.5 kcal mol^{-1}.

3.4. Dissociative Photoionization of CH_3CFCl_2 To Form CH_3CFCl^+ + Cl. Observation of only CH_3CFCl^+ with no parent ion $CH_3CFCl_2^+$ in the photoionization energy region 11.42−11.82 eV is consistent with the PIMS experiment. The broadening of CH_3CFCl^+ TOF peaks in the coincidence spectra is due to release of kinetic energy upon dissociative photoionization of CH_3CFCl_2, as explained above. In an ideal case, a single value for released kinetic energy and an isotropic distribution would give rise to a square TOF profile when the recoiling velocity of fragments is greater than that of a parent ion. A Gaussian shape of TOF peaks would be observed when the distribution of released kinetic energy is nearly Maxwellian upon dissociation of an ion. Thus, observed nearly flat-top and broadened TOF profiles imply that the distribution of kinetic energy of CH_3CFCl^+ is narrow, characteristic of a repulsive potential energy surface for the dissociation of $CH_3CFCl_2^+$ into CH_3CFCl^+.

TABLE 2: Ionization Energies (IE) of CH_3CFCl_2 and CH_3CFCl and Heats of Formation ($\Delta_fH_0^\circ$) for CH_3CFCl_2, $CH_3CFCl_2^+$, CH_3CFCl, and CH_3CFCl^+ Derived from Calculations of Isodesmic Reactions Based on G3B3 Theory, and Literature Values of $\Delta_fH_0^\circ$ for Relevant Species

		ΔH° or IE	literature $\Delta_fH_0^\circ$ [a]		derived $\Delta_fH_0^\circ$ [a]	
	equations	/kcal mol^{-1}	species	/kcal mol^{-1}	species	/kcal mol^{-1}
1	$CH_2ClCH_2Cl + {}^1/_4\,CF_4 \rightarrow CH_3CFCl_2 + {}^1/_4\,CH_4$	$\Delta H^\circ = 2.0$	CH_2ClCH_2Cl	−29	CH_3CFCl_2	−78.4
			CF_4	−221.6[b]		
			CH_4	−16.0[b]		
2	$CH_3CH_3 + {}^1/_2\,CCl_4 + {}^1/_4\,CF_4 \rightarrow CH_3CFCl_2 + {}^3/_4\,CH_4$	$\Delta H^\circ = -6.4$	CH_3CH_3	−16.4	CH_3CFCl_2	−77.4
			CCl_4	−22.4[b]		
3	$CH_3CH_2 + {}^1/_4\,CCl_4 + {}^1/_4\,CF_4 \rightarrow CH_3CClF + {}^1/_2\,CH_4$	$\Delta H^\circ = -0.4$	CH_3CH_2	31.1	CH_3CFCl	−22.3
4	$CH_3CFCl_2 \rightarrow CH_3CFCl_2^+ + e^-$	IE = 255.1	CH_3CFCl_2	−77.9[c]	$CH_3CFCl_2^+$	177.2
5	$CH_3CFCl \rightarrow CH_3CFCl^+ + e^-$	IE = 173.8	CH_3CFCl	−22.3	CH_3CFCl^+	151.5

[a] Reference 35, unless stated otherwise. [b] Reference 34. [c] An average value of $\Delta_fH_0^\circ(CH_3CFCl_2)$ from reactions 1 and 2 was used.

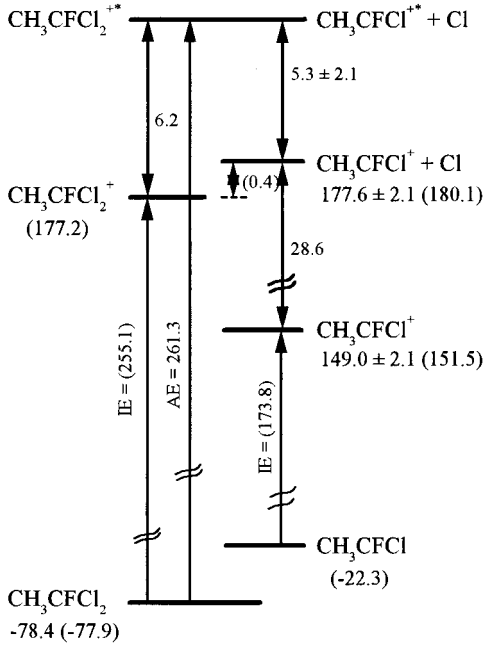

Figure 4. Schematic energy diagram for dissociative photoionization of CH_3CFCl_2 to form $CH_3CFCl^+ + Cl$ based on experimental and calculated results; the values are in kcal mol^{-1}, and calculated $\Delta_fH_0^\circ$ or IE are listed in parentheses.

Figure 4 shows an energy diagram for dissociative photoionization of CH_3CFCl_2 to form $CH_3CFCl^+ + Cl$ based on experimental and calculated results; calculated $\Delta_fH_0^\circ$ or IE are listed in parentheses. The experimentally determined thermochemical threshold for $CH_3CFCl^+ + Cl$ channel is 11.10 ± 0.09 eV (256.0 ± 2.1 kcal mol^{-1}), and accordingly the energy of this channel is 177.6 kcal mol^{-1} using $\Delta_fH_0^\circ(Cl) = 28.6$ kcal mol^{-1} and $\Delta_fH_0^\circ(CH_3CFCl_2) = -78.4$ kcal mol^{-1}. The theoretically predicted $\Delta_fH_0^\circ(CH_3CFCl_2^+)$ is 177.2 kcal mol^{-1}. The variation of 0.4 kcal mol^{-1} between energies of $CH_3CFCl_2^+$ and $CH_3CFCl^+ + Cl$ is smaller than uncertainties in experiments and theoretical calculations. Hence, we conclude that the dissociation process

$$CH_3CFCl_2^+ \rightarrow CH_3CFCl^+ + Cl \qquad (8)$$

is nearly thermoneutral.

Alternatively, the energy of $CH_3CFCl^+ + Cl$ can be estimated from ionization of CH_3CFCl. Combining predicted values of $\Delta_fH_0^\circ(CH_3CFCl) = -22.3$ kcal mol^{-1}, IE (CH_3CFCl) = 173.8 kcal mol^{-1}, and $\Delta_fH_0^\circ(Cl) = 28.6$ kcal mol^{-1}, we obtain an energy of 180.1 kcal mol^{-1} for $CH_3CFCl^+ + Cl$. This value is greater than the value 177.6 kcal mol^{-1} by 2.5 kcal mol^{-1}, but still within possible error limits of experiments and calculations. Both experimental and predicted values of the energy of $CH_3CFCl^+ + Cl$ are slighter greater than 177.2 kcal mol^{-1} predicted for $\Delta_fH_0^\circ(CH_3CFCl_2^+)$, indicating that reaction 8 is perhaps slightly endothermic.

An appearance onset of 11.33 eV (261.3 kcal mol^{-1}) for CH_3CFCl^+, about 6.2 kcal mol^{-1} above the predicted IE of 255.1 kcal mol^{-1} for CH_3CFCl_2, was determined in the PIMS experiments. According to calculations, geometries of CH_3CFCl_2 and $CH_3CFCl_2^+$ differ significantly; C−Cl bond lengths of CH_3CFCl_2 and $CH_3CFCl_2^+$ are 1.80 and 1.85 Å, and Cl−C−Cl angles are 122.0° and 100.4°, respectively, as shown in Figure 3. Detection of a KE_T of 0.23 eV (5.3 kcal mol^{-1}) at the appearance onset of CH_3CFCl^+ and observation of only CH_3CFCl^+ with no $CH_3CFCl_2^+$ also support that reaction 8 is nearly thermoneutral or slightly endothermic, and that $CH_3CFCl_2^+$, produced immediately after CH_3CFCl_2 absorbs a VUV photon, undergoes dissociation to form CH_3CFCl^+.

Similar phenomena were observed for SF_6^+ and CF_4^+ by Creasey et al. In these cases, the parent ions are virtually undetectable because their ground states are repulsive and lie above the lowest dissociation channel.[39,40] Creasey et al. found that, for SF_6^+, excess energies above the dissociation threshold are partitioned into translational energy and internal energy of fragments via a direct and rapid dissociation path; for this reason statistical methods cannot be applied to model the energy distribution. Our observed nearly flat-top and broadened TOF profiles are consistent with their observation.

4. Conclusions

With a threshold photoelectron photoion coincidence technique in pulsed mode, we investigated the formation of CH_3CFCl^+ upon photoionization of CH_3CFCl_2 at photon energies near the appearance onset of CH_3CFCl^+. After correction of maximal kinetic energy releases determined from half-widths of $CH_3CF^{35}Cl^+$ TOF peaks in coincidence spectra, we derive a thermochemical threshold at 11.10 ± 0.09 eV for the $CH_3CFCl^+ + Cl$ channel, a maximal kinetic energy release of 0.23 eV at the appearance onset of CH_3CFCl^+, and $\Delta_fH_0^\circ(CH_3CFCl^+) = 149.0 \pm 2.1$ kcal mol^{-1}. Enthalpy changes of three isodesmic reactions related to formation of CH_3CFCl_2 and CH_3CFCl, and ionization energies of CH_3CFCl_2 and CH_3CFCl, were also computed to derive heats of formation of CH_3CFCl_2, CH_3CFCl, and their corresponding cations; observed $\Delta_fH_0^\circ(CH_3CFCl^+)$ agrees satisfactorily with calculation. An energy diagram is constructed to rationalize the dissociative photoionization of CH_3CFCl_2 near the threshold region. Dissociation of $CH_3CFCl_2^+$ into $CH_3CFCl^+ + Cl$ is nearly thermoneutral, perhaps slightly endothermic; the excess energy in $CH_3CFCl_2^+$ produced im-

mediately after photoionization facilitates dissociation, consistent with lack of observation of $CH_3CFCl_2^+$.

Acknowledgment. We thank the Synchrotron Radiation Research Center and the National Science Council of Taiwan for financial support of this work (contract no. NSC89-2113-M-213-008) and the National Center for High-performance Computing for providing computing time for theoretical calculations.

References and Notes

(1) Schauffler, S. M.; Pollock, W. H.; Atlas, E. L.; Heidt, L. E.; Daniel, J. S. *Geophys. Res. Lett.* **1995**, *22*, 819.

(2) Gehring, D. G.; Barsotti, D. J.; Gibbon, H. E. *J. Chromatogr. Sci.* **1992**, *30*, 301.

(3) Talukdar, R.; Mellouki, A.; Gierczak, T.; Burkholder, J. B.; McKeen, S. A.; Ravishankara, A. R. *J. Phys. Chem.* **1991**, *95*, 5815.

(4) Fahr, A.; Braun, W.; Kurylo, M. J. *J. Geophys. Res.* **1993**, *98*, 20467.

(5) Gillotay, D.; Simon, P. C.; Brasseur, G. *Planet. Space Sci.* **1989**, *37*, 105.

(6) Melchior, A.; Bar, I.; Rosenwaks, S. *J. Chem. Phys.* **1997**, *107*, 8476.

(7) Melchior, A.; Chen, X.; Bar, I.; Rosenwaks, S. *Chem. Phys. Lett.* **1999**, *315*, 421.

(8) Huder, K.; DeMore, W. B. *Geophys. Res. Lett.* **1993**, *20*, 1575.

(9) Liu, R. Z.; Huie, R. E.; Kurylo, M. J. *J. Phys. Chem.* **1990**, *94*, 3247.

(10) Zhang, Z. Y.; Huie, R. E.; Kurylo, M. J. *J. Phys. Chem.* **1992**, *96*, 1533.

(11) Warren, R.; Gierczak, T.; Ravishankara, A. R. *Chem. Phys. Lett.* **1991**, *183*, 403.

(12) Tuazon, E. C.; Atkinson, R.; Corchnoy, S. B. *Int. J. Chem. Kinet.* **1992**, *24*, 639.

(13) Sawerysyn, J. P.; Talhaoui, A.; Meriaux, B.; Devolder, P. *Chem. Phys. Lett.* **1992**, *198*, 197.

(14) Talhaoui, A.; Louis, F.; Devolder, P.; Meriaux, B.; Sawerysyn, J.-P.; Rayez, M.-T.; Rayez, J.-C. *J. Phys. Chem.* **1996**, *100*, 13531.

(15) Tuazon, E. C.; Atkinson, R. *J. Atmos. Chem.* **1993**, *17*, 179.

(16) Warren, R. F.; Ravishankara, A. R. *Int. J. Chem. Kinet.* **1993**, *25*, 833.

(17) Chiang, S.-Y.; Wang, T.-T.; Yu, J.-S. K.; Yu, C.-h. *Chem. Phys. Lett.* **2000**, *329*, 185.

(18) Tsai, B. P.; Baer, T.; Werner, A. S.; Lin, S. F. *J. Phys. Chem.* **1975**, *79*, 570.

(19) Shiromaru, H.; Achiba, Y.; Kimura, K.; Lee, Y. T. *J. Phys. Chem.* **1987**, *91*, 17.

(20) Baer, T. *Adv. Chem. Phys.* **1986**, *64*, 111.

(21) Mayer, P. M.; Baer, T. *Chem. Phys. Lett.* **1996**, *261*, 155.

(22) Evans, M.; Ng, C. Y.; Hsu, C.-W.; Heimann, P. *J. Chem. Phys.* **1997**, *106*, 978.

(23) Cheung, Y. S.; Chen, Y.-J.; Ng, C. Y.; Chiu, S. W.; Li, W.-K. *J. Am. Chem. Soc.* **1995**, *117*, 9725.

(24) Curtiss, L. A.; Raghavachari, K.; Pople, J. A. *J. Chem. Phys.* **1993**, *98*, 1293.

(25) Chiang, S.-Y.; Ma, C.-I. *J. Phys. Chem. A.* **2000**, *104*, 1991.

(26) Frisch, M. J.; Trucks, G. W.; Schlegel, H. B.; Scuseria, G. E.; Robb, M. A.; Cheeseman, J. R.; Zakrzewski, V. G.; Montgomery, J. A. Jr.; Stratmann, R. E.; Burant, J. C.; Dapprich, S.; Millam, J. M.; Daniels, A. D.; Kudin, K. N.; Strain, M. C.; Farkas, O.; Tomasi, J.; Barone, V.; Cossi, M.; Cammi, R.; Mennucci, B.; Pomelli, C.; Adamo, C.; Clifford, S.; Ochterski, J.; Petersson, G. A.; Ayala, P. Y.; Cui, Q.; Morokuma, K.; Malick, D. K.; Rabuck, A. D.; Raghavachari, K.; Foresman, J. B.; Cioslowski, J.; Ortiz, J. V.; Baboul, A. G.; Stefanov, B. B.; Liu, G.; Liashenko, A.; Piskorz, P.; Komaromi, I.; Gomperts, R.; Martin, R. L.; Fox, D. J.; Keith, T.; Al-Laham, M. A.; Peng, C. Y.; Nanayakkara, A.; Gonzalez, C.; Challacombe, M.; Gill, P. M. W.; Johnson, B.; Chen, W.; Wong, M. W.; Andres, J. L.; Gonzalez, C.; Head-Gordon, M.; Replogle, E. S.; Pople, J. A. *Gaussian 98* (Revision A.7); Gaussian Inc.: Pittsburgh, PA, 1998.

(27) Schlegel, H. B. *J. Comput. Chem.* **1982**, *3*, 214.

(28) Becke, A. D. *J. Chem. Phys.* **1993**, *98*, 5648.

(29) Stephens, P. J.; Devlin, F. J.; Chabalowski, C. F.; Frisch, M. J. *J. Phys. Chem.* **1994**, *98*, 11623.

(30) Becke, A. D. *Phys. Rev. A* **1988**, *38*, 3098.

(31) Lee, C. T.; Yang, W. T.; Parr, R. G. *Phys. Rev. B* **1988**, *37*, 785.

(32) Dunning, T. H. *J. Chem. Phys.* **1989**, *90*, 1007. Woon, D. E.; Dunning, T. H., Jr. *J. Chem. Phys.* **1993**, *98*, 1358.

(33) Baboul, A. G.; Curtiss, L. A.; Redfern, P. C.; Raghavachari, K. *J. Chem. Phys.* **1999**, *110*, 7650.

(34) Atkinson, R.; Baulch, D. L.; Cox, R. A.; Hampson, R. F.; Kerr, J. A., Jr.; Troe, J. *J. Phys. Chem. Ref. Data* **1992**, Suppl. No. 4.

(35) Lias, G.; Bartmess, J. E.; Holmes, J. L.; Levine, R. D.; Mallard, W. G. *J. Phys. Chem. Ref. Data* **1988**, *17*, Suppl. No. 1.

(36) Kuramshina, G. M.; Weinhold, F.; Pentin, Y. A. *J. Chem. Phys.* **1998**, *109*, 7286.

(37) Melius, C. F. Sandia National Laboratories, *BAC-MP4 Heats of Formation Data File*, 1997.

(38) Curtiss, L. A.; Raghavachari, K.; Redfern, P. C.; Pople, J. A. *J. Chem. Phys.* **2000**, *112*, 7374.

(39) Creasey, J. C.; Lambert, I. R.; Tuckett, R. P.; Codling, K.; Frasinski, L. J.; Hatherly, P. A.; Stankiewicz, M. *J. Chem. Soc., Faraday Trans.* **1991**, *87*, 1287.

(40) Creasey, J. C.; Lambert, I. R.; Tuckett, R. P.; Codling, K.; Frasinski, L. J.; Hatherly, P. A.; Stankiewicz, M.; Holland, D. M. P. *J. Chem. Phys.* **1990**, *93*, 3295.